Clinical Ophthalmology

Dovepress
open access to scientific and medical research

Open Access Full Text Article

ORIGINAL RESEARCH

Characterizing Macular Neovascularization in Myopic Macular Degeneration and Age-Related Macular Degeneration Using Swept Source OCTA

Diane N Sayah[1–3], Itika Garg[1,2], Raviv Katz[1,2], Ying Zhu[1,4], Ying Cui[1,5], Rebecca Zeng[1,2], Rachel Tandias[1,2], Jade Y Moon[1,2], Filippos Vingopoulos[1,2], Hannah E Wescott[1,2], Grace Baldwin[1,2], Kira Wang[1,2], Tobias Elze[1,2], Cassie Ann Ludwig[1,2], Demetrios G Vavvas[1,2], Joan W Miller[1,2], Deeba Husain[1,2], Leo A Kim[1,2], Nimesh A Patel[1,2], John B Miller[1,2]

[1]Harvard Retinal Imaging Lab, Boston, MA, USA; [2]Retina Service, Department of Ophthalmology, Massachusetts Eye and Ear, Harvard Medical School, Boston, MA, USA; [3]College of Optometry, University of Houston, Houston, TX, USA; [4]Eye Center of Xiangya Hospital, Central South University, Changsha, Hunan, People's Republic of China; [5]Guangdong Eye Institute, Department of Ophthalmology, Guangdong Provincial People's Hospital, Guangdong Academy of Medical Sciences, Guangzhou, People's Republic of China

Correspondence: John B Miller, Retina Service, Massachusetts Eye and Ear, Department of Ophthalmology, Harvard Medical School, 243 Charles St, Boston, MA, 02114, USA, Tel +1 617 573-3750, Fax + 1 617 573-3698, Email John_Miller@meei.harvard.edu

Purpose: Visual prognosis and treatment burden for macular neovascularization (MNV) can differ between myopic macular degeneration (MMD) and age-related macular degeneration (AMD). We describe and compare MNV associated with MMD and AMD using swept-source (SS)-OCTA.

Patients and Methods: Adult patients with documented MNV associated with MMD or AMD were consecutively recruited. Qualitative and quantitative features were assessed from 6x6mm angiograms, including the MNV area and vessel density (VD). Descriptive statistics and linear regression analyses were carried out.

Results: Out of 75 enrolled eyes with diagnosed MNV (30 MMD-MNV and 45 AMD-MNV; mean age 55±19 and 75±8 years, respectively), 44 eyes had discernible MNV (11 MMD-MNV and 33 AMD-MNV) on SS-OCTA at the time of the study and were included in the analysis. The MMD-MNV group exhibited a three-fold smaller sized MNV ($p=0.001$), lower greatest linear dimension ($p=0.009$) and greatest vascular caliber ($p<0.001$) compared to AMD-MNVs, and had a higher prevalence of tree-in-bud pattern. Eyes with AMD showed a higher prevalence of type 1 MNVs with medusa pattern. There was no difference in the location of the MNV, shape's regularity, margins, presence of core vessel, capillary fringe, peripheral loops, or perilesional dark halo ($p>0.05$) between both conditions. After adjustment, decreased MNV area and increased VD were associated with the tree-in-bud pattern, whereas the diagnosis did not significantly influence those parameters.

Conclusion: While larger studies are warranted, this study is the first to describe and compare MMD-MNV and AMD-MNV using SS-OCTA, providing relevant clinical insight on MNV secondary to MMD and AMD. These findings also further validate OCTA as a powerful tool to detect and characterize MNV non-invasively.

Keywords: macular neovascularization, age-related macular degeneration, high myopia, swept source, OCT angiography

Introduction

Macular neovascularization (MNV) is an invasion of the macular area by abnormal blood vessels, which grow and proliferate in response to angiogenic stimuli in or below the retina.[1] Many diseases of the eye can be associated with MNV, including myopic macular degeneration (MMD) and age-related macular degeneration (AMD), which are leading causes of significant visual impairment in developed countries in younger and older adults, respectively.[2,3]

While classical features of each of these disease entities (such as the presence of a myopic fundus or drusen) may help clinicians distinguish them, very few studies have compared the characteristics of MNVs associated with MMD to those associated with AMD.

Received: 11 October 2023
Accepted: 27 November 2023
Published: 12 December 2023

The recent emergence of OCT angiography (OCTA), an imaging technology based on diffractive particle movement detection, generates high-resolution three-dimensional reconstruction of blood vessels in the retina and choroid without the use of injected dye. A growing body of evidence attests to the ability of OCTA to distinguish MNV features associated with different ocular diseases. For example, MNV networks secondary to white-dot syndromes were found to be smaller than those secondary to AMD, but had a similar vessel density.[4] The morphology and characteristics of MNVs secondary to MMD and those secondary to AMD have not been previously described using optical coherence tomography angiography (OCTA). This is relevant to better understand MNV pathophysiology in these disease processes, and especially important in clinical decision-making since visual prognosis and treatment burden for MNV differ between MMD and AMD.[5] Anti-vascular endothelial growth factor (anti-VEGF) injections are a common and efficacious treatment for MNV; however, sustained regression of MNV often occurs with only one to two injections in MMD as opposed to MNV in AMD, which can require injections throughout a patient's lifetime once diagnosed.

The objective of this study is to describe and compare features of MNV secondary to MMD with those secondary to AMD using swept-source (SS)-OCTA, highlighting features that may be helpful in guiding clinical practice.

Materials and Methods

Study Cohort

This prospective cross-sectional study was approved by the Massachusetts Eye and Ear Infirmary Institutional Review Board (2019P001863) and conformed to the principles of the Declaration of Helsinki and Health Insurance Portability and Accountability Act regulations. Patients were consecutively recruited from the Ophthalmology Retina Service, and testing was performed after obtaining detailed informed written consent.

All participants underwent a comprehensive ophthalmologic examination by experienced, board-certified retina specialists on the same visit as SS-OCTA imaging. Adult patients (≥18 years of age) with a confirmed diagnosis of MNV associated with either MMD or AMD on clinical examination were recruited. Diagnostic criteria included best-corrected visual acuity, dilated slit-lamp examination, OCT imaging, FA and/or ICGA when deemed necessary, and OCTA.

Medical records were reviewed to obtain best corrected visual acuity (BCVA) at the imaging visit in Logarithm of the Minimum Angle of Resolution (logMAR), lens status, intraocular pressure (IOP) in mm Hg measured using the Tono-Pen (Reichert Technologies, Depew, NY), course of intravitreal injection (IVI) therapy administered, currently administered anti-VEGF agents, previous photodynamic therapy (PDT), as well as systolic and diastolic blood pressure (SBP and DBP respectively), medical systemic history, body-mass index (BMI), and self-reported ethnicity and race according to NIH guidelines.

Subjects were included regardless of treatment status with anti-VEGF agents; more specifically, eyes with treatment-naïve MNV as well as treated or previously treated MNV were included in this study. They were excluded if their BCVA was worse than 20/400, had corneal, lens, or media opacities that resulted in poor retinal OCT quality, or had unsteady fixation. Subjects were also excluded if they had concomitant trauma or disease such as retinal vascular occlusion, optic neuropathy including glaucoma, central serous chorioretinopathy, uveitis, vitreomacular traction, and recent laser treatment or ocular surgery within the past 3 months. The presence of an epiretinal membrane with retinal distortion was also an exclusion criterion.

Imaging Protocol and Analysis

OCTA imaging was carried out using a SS-OCT device (PLEX® Elite 9000; Carl Zeiss Meditec, Dublin, CA, USA). A 6×6 mm angiogram centered on the fovea was acquired at a rate of 100,000 A-scans per second. Only images with signal strength ≥ 7 were included in this study. Following projection artifact removal, en-face outer-retina to choriocapillaris (ORCC) retinal slabs were exported using the built-in review software. The proprietary automated multilayer segmentation (MLS) algorithm was used. Retinal and choroidal boundaries were adjusted manually if the automated segmentation was deemed inaccurate. Images were excluded if they featured artifacts that would hinder image

processing, such as significant motion or gap artifacts. If anti-VEGF therapy was required on the same visit, imaging was carried out prior to IVI.

Following Otsu binarization,[6] the MNV lesion was manually delineated by a well-trained experienced grader using the freehand selection tool in FIJI (ImageJ, National Institute of Health, Bethesda, MD, USA).[7] If the lesion was ill-defined, information from the b-scan and en-face OCTA scans was used to help delineate the MNV. The MNV outline was saved as a region of interest (ROI) and the outer selection was converted to a black background using the "clear outside" command in FIJI. The MNV network was quantified using AngioTool 0.6a,[8] a validated semi-automated open-source software, after careful optimization of parameters to best resolve the vascular network. The MNV area and vessel density, vessel length, branching index (calculated as the number of junctions divided by the area of the lesion), and the lacunarity were thus obtained. The greatest vascular caliber (GVC), defined as the diameter of the MNV's largest vessel or trunk vessel if applicable, was delimitated and measured using the straight-line tool in FIJI. Similarly, the greatest linear dimension (GLD) of the lesion on OCTA was measured and recorded as the length in mm and the orientation in degrees.

Several qualitative features of the MNV were assessed in this study, including the depth, location, shape, margins, and the presence of a core vessel, capillary fringe, peripheral loops, and perilesional dark halo. MNV depth was classified according to established classification: Type 1 MNV represents areas of neovascularization below the retinal pigment epithelium (RPE); type 2 MNV is located in the subretinal space, above the RPE; mixed type is located in the subretinal and sub-RPE space; and type 3 MNV, also defined as retinal angiomatous proliferation, presents neovascularization developed within the neurosensory retina.[1] If any ambiguity, open adjudication between two graders was performed to reach consensus. The location of the MNV was classified as subfoveal or foveal sparing. The vascular network's morphology was described in terms of the regularity of its shape (round vs irregular) and the overall pattern of the MNV. The "medusa" pattern represents a lesion where vessels radiate in all directions from the center, the "sea-fan" pattern, where vessels radiated in all directions from one side, and the "tree-in-bud", a round lesion without obvious vascular trunk, as described elsewhere[9,10] and as illustrated in the figure the MNV lesions' margins were characterized as being well or poorly defined on the basis of appearance. Additional important features such as the presence of a capillary fringe, the presence of peripheral loops, the presence of a perilesional dark halo, and the presence of a core vessel were also recorded (see Figure 1).

Finally, MNV activity was classified as active (visual loss, leakage on FA, intraretinal or subretinal exudation on OCT, anti-VEGF injection intervals <12 weeks), silent (defined as treatment-free interval ≥ 3 months), or quiescent (MNV with absence of intraretinal or subretinal exudation on repeated OCTs) for eyes with AMD-MNV, and in the active, scar or atrophic stages for MMD-MNV based on fundoscopic and OCT findings as previously described.[10–12]

Statistical Analysis

Statistical analyses were performed using SPSS statistical software (version 27; SPSS, Inc., Chicago, IL). Traditional descriptive methods were used to analyze baseline demographics and clinical characteristics. Using linear regression models, our statistical approach was centered on MNV area and VD. We used a stepwise regression using both forward and backward selection to achieve the multivariate models presented for MNV area and VD. For all statistical tests, p-values ≤ 0.05 were considered significant.

Results

Seventy-five eyes (66 subjects) with confirmed MNV were included in the study. A description of their baseline characteristics is presented in Table 1.

Thirty eyes (25 subjects) had MMD-MNV (mean RE of −12.51D) and 45 eyes (41 subjects) had AMD-MNV (mean RE of +0.55D). BCVA was similar in both groups. Subjects in the MMD-MNV group were significantly younger than those in the AMD-MNV group (55 vs 75 years). Both groups were composed of significantly more females than males (p=0.030). While a majority of patients were "White" in both groups, the MMD-MNV group was more diverse, comprising 8% (2) of participants from Asian origin and 20% (5) from Hispanic origin.

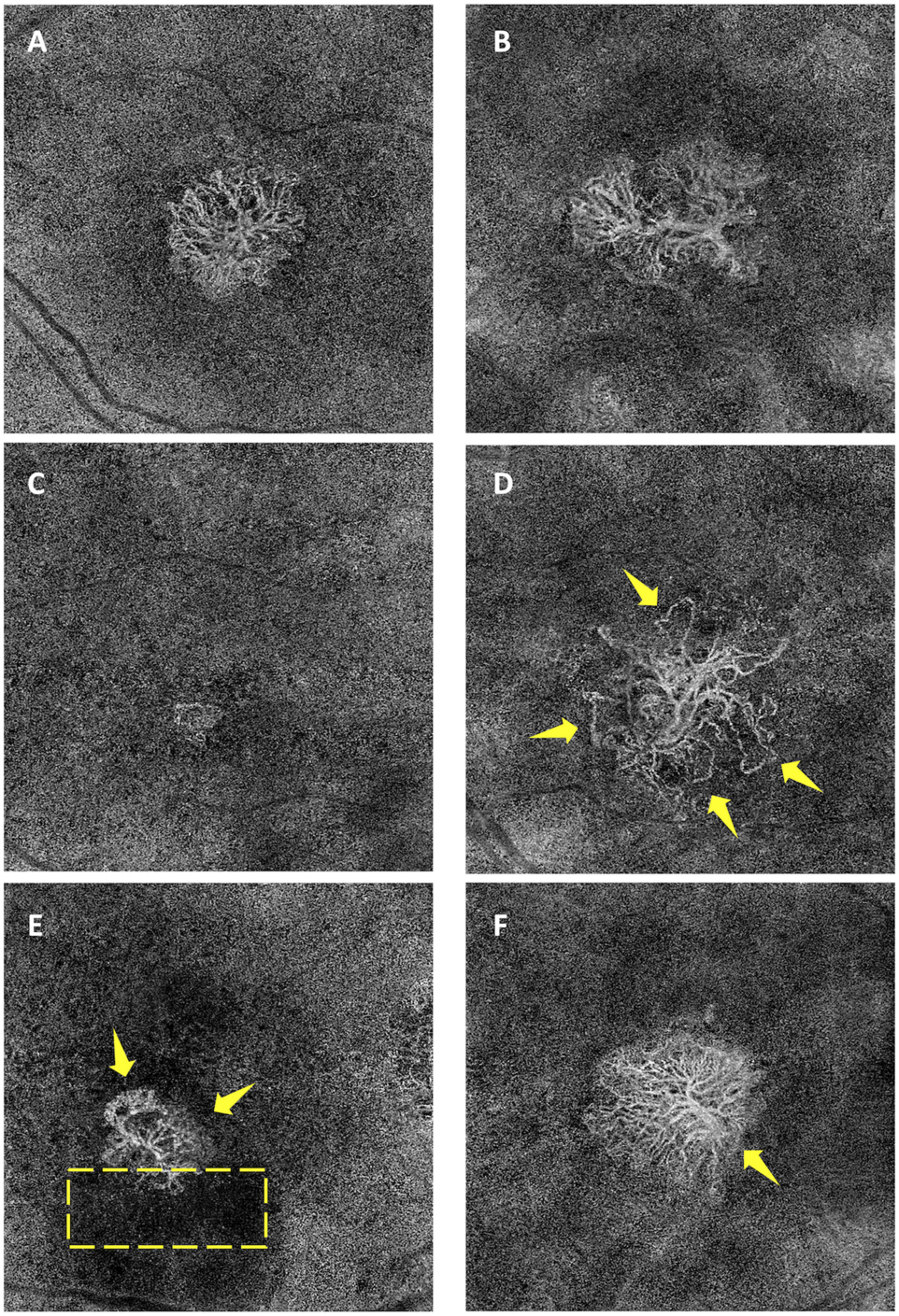

Figure 1 Morphologic patterns of macular neovascularization (MNV) as visualized using swept-source OCT Angiography. Shape descriptors included (**A**) the "Medusa" pattern representing a lesion where vessels radiate in all directions; (**B**) the "Sea-fan" pattern representing a lesion where blood vessels radiate in all directions from one side; and (**C**) the "Tree-in-bud" pattern representing a round lesion with no obvious vascular trunk. Images were also evaluated for the presence of (**D**) peripheral loops (indicated by the yellow arrows), (**E**) capillary fringe (indicated by the yellow arrows), a perilesional dark halo (indicated by the box) and (**F**) a core vessel (indicated by the yellow arrows).

Eyes in the MMD group were administered a significantly lower number of total IVIs (5±7 vs 14±11 in the MMD and AMD groups, respectively, p<0.001), presented with a greater duration between the last therapeutic IVI and the imaging visit (p=0.002), and only 37% were actively treated with IVIs on the imaging date as opposed to 71% in the AMD group (p=0.003).

Table 1 Summary of Demographic and Clinical Characteristics for Eyes with MNV Secondary to Myopic Macular Degeneration (MMD) and Eyes with MNV Secondary to Age-Related Macular Degeneration (AMD)

		MMD (n=30 Eyes; 25 Subjects)	AMD (n=45 Eyes; 41 Subjects)	p-value
Male (%)		3/25 (12)	15/41 (37)	**0.030**
Age (years)		55±19	75±8	**<0.001**
Racial/Ethnic background	Asian (%)	2/25 (8)	0/41 (0)	**0.002**
	Hispanic or Latino (%)	5/25 (20)	0/41 (0)	
	White (%)	17/25 (68)	38/41 (93)	
	Undeclared (%)	1/25 (4)	3/41 (7)	
Systemic blood pressure	Systolic (mm Hg)	131±25	131±15	0.998
	Diastolic (mmHg)	75±11	74±10	0.883
Smoking status	Current	1/25 (4)	2/41 (5)	0.118
	Never	18/25 (72)	19/41 (46)	
	Former	6/25 (24)	20/41 (49)	
Body-mass index		26.3±5.0	28.4±5.0	0.145
LogMAR BCVA		0.31±0.35 (~20/40)	0.30±0.26 (~20/40)	0.954
Spherical equivalent (diopter)		−12.51±5.09	+0.55±1.59	**<0.001**
Previous PDT		3/30 (10)	2/45 (4)	0.345
Number of prior anti-VEGF injections		5±7	14±11	**<0.001**
Time since last injection (months)		27±36	4±9	**0.002**
Treatment naive		3/30 (10)	7/45 (16)	0.488
Treated with:	Aflibercept	6/30 (20)	20/45 (44)	0.066
	Bevacizumab	14/30 (47)	8/45 (18)	
	Ranibizumab	6/30 (20)	8/45 (18)	
	Not specified	1/30 (3)	3/45 (7)	
Actively getting IVI therapy (%)		11/30 (37)	32/45 (71)	**0.003**
Intraocular pressure (mm Hg)		16.2±3.4	15.7±3.4	0.545
Lens status	Phakic	23/30 (77)	23/45 (51)	**0.026**
	Pseudophakic	7/30 (23)	22/45 (49)	

Notes: The data is presented as mean ± standard deviation where applicable. The data in parentheses is presented as a percentage (%), and significant p-values (<0.05) are highlighted in bold.

Unfortunately, out of the 75 eyes, only 44 eyes had discernible MNVs on en-face SS-OCTA, despite a confirmed clinical diagnosis of MNV. As summarized in Table 2, of those 44 eyes with discernible MNVs, we found a large proportion (94%) of type 1 MNVs secondary to AMD, while 6 (55%) and 4 (36%) of MMD-MNVs were of types 1 and 2, respectively. Morphologically, a majority of AMD-MNVs (52%) resembled the medusa pattern and MMD-MNVs (55%) resembled the tree-in-bud pattern. There was no difference in the location of the MNV, the shape's regularity, the

Table 2 Summary of Qualitative and Quantitative Assessment of MNV Morphology Secondary to Myopic Macular Degeneration (MMD) and Age-Related Macular Degeneration (AMD) Using SS-OCTA

		MMD n=11 Eyes	AMD n=33 Eyes	p-value
MNV type	1	6/11 (55)	31/33 (94)	**0.006**
	2	4/11 (36)	1/33 (3)	
	3	1/11 (9)	1/33 (3)	
Location	Subfoveal	8/11 (73)	24/33 (73)	1.000
	Foveal sparing	3/11 (27)	9/33 (27)	
MNV activity[a]	Active	6/11 (55)	26/33 (79)	**0.018**
	Scar	4/11 (36)	–	–
	Atrophic	1/11 (9)	–	–
	Silent	–	6/33 (18)	–
	Quiescent	–	1/33 (3)	–
Shape	Round	6/11 (55)	14/33 (42)	0.484
	Irregular	5/11 (45)	19/33 (58)	
Pattern	Medusa	3/11 (27)	17/33 (52)	**0.033**
	Sea-fan	2/11 (18)	11/33 (33)	
	Tree-in-bud	6/11 (55)	5/33 (15)	
Well-defined margins		7/11 (64)	26/33 (79)	0.315
Presence of a core vessel		1/11 (9)	8/33 (24)	0.281
Presence of capillary fringe		4/11 (36)	18/33 (55)	0.296
Presence of perilesional dark halo		3/11 (27)	13/33 (39)	0.469
Presence of peripheral loops/arcades		8/11 (73)	28/33 (85)	0.367
Greatest linear dimension	Length (mm)	1.41±0.90	2.44±1.38	**0.009**
	Angle (degrees)	−15.0±83.1	−34.2±61.3	0.491
Greatest vascular caliber (mm)		0.038±0.012	0.067±0.041	**<0.001**
MNV area (mm^2)		1.38±1.53	4.73±4.86	**0.001**
Vessel density (%)		51.7±14.9	42.0±11.7	0.071
Branching Index		69.5±48.5	47.3±28.5	0.175
Total vessels length		12.5±12.6	36.0±33.8	**0.002**
Mean vessels length		6.39±10.16	4.40±3.67	0.537
Mean lacunarity		0.197±0.111	0.205±0.121	0.844

Notes: [a]MNV activity was classified as active, silent (treatment-free interval ≥ 3 months) or quiescent (or treatment-naïve) for eyes with AMD-MNV and in the active, scar or atrophic stages for MMD-MNV based on established criteria.[10–12] The data is presented as mean ± standard deviation where applicable. The data in parentheses is presented as a percentage (%), and significant p-values (<0.05) are highlighted in bold.

presence of a core vessel, a capillary fringe, well-defined margins, peripheral loops, or a perilesional dark halo between both conditions ($p > 0.05$).

The size of AMD-MNV lesions was significantly larger (in area and GLD) than those in MMD-MNV (4.73 ±4.86 mm^2 vs 1.38±1.53 mm^2, and 2.44±1.38 mm vs 1.41±0.90 mm, respectively). The GVC was superior in AMD eyes than in MMD, as was the total vessel length within the lesion, but not the mean vessel length when adjusted for lesion size. There was a tendency for greater VD in the MMD-MNV group.

Univariate analyses for MNV area and VD are shown in Table 3. Using stepwise regression, the best model for the MNV area (adjusted R^2=0.21) included the tree-in-bud MNV pattern (ß=−3.99, 95% CI [−7.46, −0.51], p=0.026). In other words, compared to the medusa pattern, the tree-in-bud pattern significantly decreased the MNV area by 3.99 mm^2 while controlling for sex and refractive error. The best model for VD (adjusted R^2=0.28) included the tree-in-bud pattern (ß=15.58, 95% CI [6.74, −24.43], p=0.001), indicating a 15.58% increase in VD in the tree-in-bud pattern compared with the medusa pattern. The diagnosis (MMD vs AMD) did not show significance for the MNV area or VD after adjustment.

Out of ten treatment naïve eyes (3 with MMD; 7 with AMD) in this study, 1 MNV in the MMD group and 6 MNVs in the AMD group were discernible on en-face SS-OCTA. These eyes featured round MNVs, well-defined margins, and no core vessel. Their detailed characteristics are summarized in Table 4. Of interest, 70% of treatment-naïve eyes had discernible MNVs compared with 57% of treated eyes; however, this difference was not statistically significant (p=0.434).

Table 3 Univariate Regression Analysis of MNV Area and Vessel Density

	MNV Area			**MNV Vessel Density**		
	ß Coefficient	**95% CI**	**p-value**	**ß Coefficient**	**95% CI**	**p-value**
Sex	1.60	−1.69 to 4.89	0.332	2.88	−6.77 to 12.53	0.550
Age	0.081	0.002 to 0.16	**0.045**	−0.30	−0.52 to −0.08	**0.009**
Racial/Ethnic background	−0.43	−2.33 to 1.47	0.649	−1.31	−6.84 to 4.22	0.635
SBP	0.054	−0.28 to 0.14	0.186	−0.19	−0.43 to 0.44	0.108
DBP	0.012	−0.14 to 0.17	0.872	−0.12	−0.56 to 0.33	0.590
Smoking status	3.09	0.80 to 5.38	**0.010**	−4.11	−11.24 to 3.02	0.251
BMI	−0.21	−0.53 to 0.11	0.189	0.43	−0.50 to 1.36	0.355
LogMAR VA	4.75	0.28 to 9.22	**0.038**	−16.61	−29.31 to −3.91	**0.012**
Refractive Error	0.25	0.04 to 0.46	**0.022**	−0.68	−1.30 to −0.05	**0.035**
Prior PDT	−9.13	−13.94 to −4.32	**<0.001**	4.59	−11.61 to 20.80	0.570
Nb of prior IVIs	0.18	0.033 to 0.32	**0.018**	−0.29	−0.73 to 0.15	0.191
Time since last IVI	−0.035	−0.88 to 0.018	0.185	0.16	0.015 to 0.31	**0.032**
Active IVI Therapy	−0.30	−3.12 to 2.52	0.831	0.18	−8.02 to 8.39	0.964
IOP	0.30	−0.14 to 0.73	0.172	−0.86	−2.11 to 0.39	0.172
Lens status	0.65	−2.21 to 3.50	0.650	−0.29	−8.62 to 8.04	0.944
MNV Type	−1.47	−4.18 to 1.25	0.283	5.90	−1.91 to 13.70	0.135
MNV Pattern	−2.03	−3.61 to −0.45	**0.013**	6.54	2.02 to 11.07	**0.006**
Diagnosis (MMD vs AMD)	2.98	0.29 to 5.67	**0.031**	−8.57	−16.41 to −0.73	**0.033**

Note: Significant p-values (<0.05) are highlighted in bold.

Abbreviations: MNV, macular neovascularization; SBP, systolic blood pressure; DBP, diastolic blood pressure; BMI, body-mass index; VA, visual acuity; PDT, photodynamic therapy; IVI, intravitreal injection; IOP, intraocular pressure; MMD, myopic macular degeneration; AMD, age-related macular degeneration.

Table 4 Characteristics of Treatment-Naïve MNVs in Eyes with Discernible Lesions on En-Face SS-OCTA

Case	Dx	LogMAR BCVA	MNV Type	Location	Active	MNV Pattern	Capillary Fringe	Peripheral Loops	Dark Halo	MNV Area (mm^2)	MNV VD (%)
1	MMD	0.90 (20/160)	2	Subfoveal	Yes	Medusa	Yes	Yes	No	2.51	51.8
2	AMD	0.00 (20/20)	1	Subfoveal	No	Medusa	Yes	Yes	No	1.58	49.1
3	AMD	0.70 (20/100)	1	Perifoveal	Yes	Medusa	Yes	Yes	No	1.77	52.0
4	AMD	0.50 (20/63)	1	Perifoveal	Yes	Medusa	Yes	Yes	Yes	1.74	31.7
5	AMD	0.48 (20/60)	1	Subfoveal	Yes	Medusa	Yes	Yes	No	11.86	48.8
6	AMD	0.60 (20/80)	2	Subfoveal	Yes	Medusa	Yes	Yes	No	6.80	33.4
7	AMD	0.1 (20/25)	3	Subfoveal	Yes	Tree-in-bud	No	No	Yes	0.069	66.3

Note: All seven cases presented with round MNVs with well-defined margins and no core vessel.

Only one subject with a discernible MNV and self-reported racial/ethnic background different than "White" was found. The subject was a young male of Hispanic origin with an inactive (scar stage), type 3 MMD-MNV. The MNV was described as subfoveal, round, tree-in-bud pattern with small peripheral loops. The MNV's area and VD were 0.064 mm^2 and 67.6%, respectively, following treatment with two bevacizumab IVIs administered 6 and 7 months, respectively, before the imaging visit.

Discussion

To our knowledge, this is the first study to describe and compare MMD-MNV to AMD-MNV as encountered in a clinical setting using SS-OCTA. In general, our cohort exhibited a larger MNV area in AMD eyes with a trend for higher VD in MMD. Stepwise linear regression demonstrated an association between a larger MNV size and the tree-in-bud pattern, as well as between a smaller VD and the same MNV pattern. While the diagnosis (MMD vs AMD) was not found to predict the MNV area and VD, our findings suggest that MMD-MNVs feature a higher prevalence of tree-in-bud pattern, which in turn is associated with a smaller MNV area and higher VD. There was a higher prevalence of type 1 (94%), medusa patterned (52%) MNVs in eyes with AMD. The GLD and GVC were also greater in AMD eyes. While the MNV lesions' vessels length was also greater in AMD eyes, this was mainly due to larger MNV area, as represented by the mean vessel length, rather than the clinical diagnosis. The branching index was higher in MMD-MNV eyes, although this was not statistically significant (p=0.175). Also, no difference in MNV location, shape regularity, or in the presence of a core vessel, capillary fringe, well-defined margins, peripheral loops, and dark perilesional halos were found between the MMD and AMD groups.

Concordance between our findings and those from previous studies further validates SS-OCTA as a powerful tool to describe and compare MNVs in eyes with various conditions.[13] For example, MNV area was previously shown to be smaller in myopes, and a predilection for type 1 MNV was associated with AMD.[14–16] While the Verteporfin in photodynamic therapy study group[17] reported that 83% of myopic MNVs were predominantly type 2, our smaller cohort showed 4 out of 11 MMD-MNV eyes to be type 2. This is contrary to earlier studies reporting the predominance of type 2 in myopic MNV, perhaps since in the scar phase MNV is enclosed by RPE,[18] or due to the small sample size of MMD-MNVs. Only one MNV was classified as type 3 in the MMD group, which is atypical. That MNV was very small in size and was previously treated with 2 anti-VEGF injections at least 18 months prior to the study visit. This MNV presented in a Hispanic male who was also presented with the highest myopic refractive error in our cohort. In another study, the location of about 23% of MMD-MNVs were classified as "juxtafoveal" or foveal sparing using FA,[19] which is consistent with our current results.

All MNVs in treatment-naïve eyes were circular, had well-defined margins and no core vessel. As described in Table 4, most of these MNVs presented subfoveally, as a medusa pattern, with capillary fringe, peripheral loops, and no perilesional dark halo. The presenting BCVA was also worse in the MMD-MNV treatment-naïve eye than in eyes with treatment-naïve AMD-MNV. Following treatment, morphological changes such as vessel pruning and regression of MNV networks are expected, while baseline neovascular patterns remain unchanged.[9,20] In our study, the number of

treatment-naïve eyes limits our ability to discuss any significant differences between untreated and treated eyes. While our observations may still provide some insight into the development of MNVs secondary to MMD and AMD, and some of their respective morphological features, further studies with larger cohorts of treatment-naïve eyes are required.

Active MNVs represented 55% of eyes with MMD compared with 79% of eyes with AMD in our study. Correspondingly, the MMD group also presented a lower number of IVIs administered and 37% (vs 71% in the AMD group) were actively undergoing therapeutic injections on the imaging visit. This is consistent with our current understanding of myopic MNV treatment – that fewer injections are typically required to treat it.[5] Longitudinal studies suggest that MMD-MNVs are usually self-limited and tend to regress without[21] or with short-duration treatment, especially in young patients.[19]

Systemic risk factors for various diseases of the eye include age, but also sex, race/ethnicity, smoking, and obesity. Subjects with MMD-MNV were generally younger than those with AMD-MNV in our cohort. Interestingly, it was previously suggested that the area of MMD-MNVs occurring in younger patients is smaller than those occurring in older patients, the latter being closer in size to AMD-MNVs.[15,19] A positive association between larger MNV area and older age (ß=0.081, p=0.045) in our study may support findings from previous reports.

We speculate that MNV morphology and size, as well as their response to treatment, may also be explained by differences in the pathophysiological mechanisms underlying MMD-MNVs and AMD-MNVs, although we do not test for this in our study. One hypothesis for the pathogenesis of MMD-MNVs is that mechanical tissue strain in myopic eyes, which present with low ocular rigidity (ie, a more compliant sclera),[22] leads to localized breaks in the RPE-Bruch's membrane (lacquer cracks) that allow for the ingrowth of new vessels.[14] In support of this theory, mechanical stress was shown to increase VEGF production by RPE cells in vitro.[23] It is generally accepted that a combination of background changes due to ocular axial elongation as well as the increase in angiogenic factors would lead to an ingrowth of MNV in high myopia.[5] However, the exact mechanism leading to MMD-MNV is not yet known, and several other factors may be involved, including choroidal thinning and genetic factors.[24–26] In exudative AMD, the causal mechanisms also remain unclear; however, it is likely that they may be immunovascular in nature and that choroidal involution would be involved.[27] Some evidence points to vessel loss and reduced perfusion in the choroid preceding the formation of pathological vessels and RPE injury,[28,29] suggesting VEGF secretion and MNV formation to occur following choroidal hypoxia.[30] It is therefore possible that morphological and size differences between MNVs (and also their response to treatment) may be a reflection of the more diffuse macular process of AMD, as opposed to a more localized process in MMD.

Both the AMD-MNV and MMD-MNV groups were associated with a female predilection (p=0.030) as expected from previous reports.[3,31] Caucasians are more likely to get AMD,[31] which is reflected in the composition of our AMD group. The MMD group included 2 Asian and 5 Hispanic patients, although only one Hispanic subject had a discernible MMD-MNV, preventing us from elaborating further on the effect of race/ethnicity on MNV morphology. Little is known on the influence of race/ethnicity on MNV, except for a documented higher prevalence of advanced AMD in white individuals,[2] and of MMD in Asians.[3] Smoking status and BMI were not different between AMD and MMD groups (p>0.05) and reflected participants who were mostly non-smokers or ex-smokers, and overweight, but not obese.

Out of 75 eyes from initially-recruited participants, 19 (63%) eyes with MMD-MNV and 12 (27%) eyes with AMD-MMD in our cohort had indiscernible MNV vascular networks using en-face OCTA, irrespective of the en-face retinal slab used and despite good signal strength (≥7). In comparison, Querques et al[32] presented only 4 of 36 eyes (11%) with myopic MNV, where the vascular network was not clearly visualized using a 3×3mm scan protocol with the Cirrus HD-OCT 5000, citing poor quality of OCT-A images due to extensive RPE and chorioretinal atrophy. Why the discrepancy? While data on the time elapsed since the last IVI is unavailable to compare, we speculate that our cohort is comprised of eyes with longer duration of time since the last IVI, representing MNVs which may have regressed following effective treatment. Another possibility worth noting is that some eyes with indiscernible MNVs on OCTA may have had idiopathic macular hemorrhage as opposed to actual MNVs.[33] In addition, while MMD-MNVs are generally of type 2 and thus expected to be better visualized due to being located above the RPE,[34] our findings do not reflect a larger proportion of type 2 MNVs in the MMD group. MMD-MNVs may understandably be harder to visualize than AMD-MNVs due to steeper curvature of the eye due to elongation, poorer segmentation of the thin retinal and choroidal layers,

and smaller sized MNVs. In turn, Eandi et al[35] reported 18.7% of eyes with indiscernible MNV in AMD, which is closer to our findings for this group.

Overall, the development of OCT-A has been revolutionary and has shown a good ability to detect MNVs non-invasively. While FA and ICGA remain valuable tools that cannot yet be supplanted in detecting leakage and investigating choroidal pathology, OCT-A has exhibited a sensitivity of 90.48% and specificity of 93.75% in detecting MMD-MNV,[32] and an overall sensitivity of 71% and specificity of 81% compared with FA in detecting AMD-MNV, central serous chorioretinopathy, and MMD in other studies.[34] Furthermore, unlike FA and ICGA, OCTA does not rely on the injection of dye to visualize vascular networks, thus eliminating the risk ofpotential adverse allergic reactions.

Major limitations of the current study include the relatively small number of eyes with classifiable MMD-MNV and the heterogeneity of our samples in terms of MNV activity and treatment duration and currency, all of which represent the reality of cases encountered in clinical settings. The reported results may thus not be entirely generalizable. We suggest that a prospective study that includes more eyes with treatment-naïve MNVs would allow us to better characterize the initial presentation of MNVs according to their etiology and understand the impact of anti-VEGF therapy on MNV morphological changes. The unavailability of ocular axial length measurements is another limitation of our study, however MNV lesions are now recognized to occur at any degree of myopia,[36] and in our cohort, all myopic eyes exhibited characteristics of a myopic fundus, suggesting eye elongation. To this effect, the underlying choroid was severely thinned in most MMD eyes, hindering further analysis of vascular density in this layer.

Conclusion

This study is the first to describe and compare MMD-MNV and AMD-MNV using SS-OCTA. In our small cohort, MMD-MNV networks were generally smaller in size but had similar VD to AMD-MNV, which may be explained by the pathophysiological mechanisms underlying the respective disease processes. While larger follow-up studies are warranted to confirm and further characterize MNVs, as well as identify characteristics that may help predict treatment response and visual prognosis, this report provides relevant insight into morphological differences for MNVs secondary to MMD and AMD for clinicians.

Abbreviations

AMD, Age-related macular degeneration; BCVA, Best-corrected visual acuity; BMI, Body-mass index; D, Diopters; DBP, Diastolic blood pressure; FA, Fluorescein angiography; GLD, greatest linear dimension of macular neovascularization network; GVC, Greatest vascular caliber of macular neovascularization network; ICGA, Indocyanine green angiography; IOP, Intraocular pressure; IVI: Intravitreal injection; LogMAR, Logarithm of the minimum angle of resolution; MLS, Multilayer segmentation; MMD, Myopic macular degeneration; MNV, Macular neovascularization; OCTA, Optical coherence tomography angiography; ORCC, Outer-retina to choriocapillaris; PDT, Photodynamic therapy; RE, Refractive error; RPE, Retinal pigment epithelium; SBP, Systolic blood pressure; SS-OCTA, Swept-source optical coherence tomography angiography; VD, Vessel density; VEGF, Vascular endothelial growth factor.

Acknowledgments

This work was supported by the Lions International Fund [Grants 530125, 530869] Lions International Fund [Grants 530125, 530869] and the National Institutes of Health [Grant P30EY003790]. The funding organizations had no role in the design or conduct of this research.

The abstract of this paper was presented at the Association for Research in Vision and Ophthalmology (ARVO) Meeting as a poster presentation with interim findings. The poster's abstract, titled "Characterizing Macular Neovascularization in Myopic Macular Degeneration and Age-related Macular Degeneration using Swept Source OCT Angiography" was published in "ARVO Annual Meeting Poster Abstracts" in Investigative Ophthalmology & Visual Science. (https://iovs.arvojournals.org/article.aspx?articleid=2779923).

Disclosure

C.A.L. has received financial support from the Ronald G. Michels Fellowship Foundation Award and the Heed Fellowship sponsored by the Society of Heed Fellows and has a patent pending related to a myopia control therapeutic. D.G.V. is a consultant for Valitor and Olix Pharmaceuticals and has received financial support from the National Eye Institute and by grants from the National Institutes of Health (R01EY025362 and R21EY0203079), Research to Prevent Blindness, Loeffler's Family Foundation, Yeatts Family Foundation, and Alcon Research Institute. J.W.M. is a consultant for Genentech/Roche, Sunovion, KalVista Pharmaceuticals, and ONL Therapeutics; received honorarium from Heidelberg Engineering; holds a patent through and has received financial support from ONL, Drusolv Therapeutics, Valeant Pharmaceuticals/Massachusetts Eye and Ear; has received financial support from Lowy Medical Research Institute, Ltd, and the National Eye Institute (R01EY03088); and holds stock options from Aptinyx and ONL Therapeutics, as well as equity from Ciendias. In addition, J.W.M. has a patent US 7,811,832 with royalties paid to ONL Therapeutics, patents US 5,798,349; US 6,225,303; US 6,610,679; CA 2,185,644; CA 2,536,069 with royalties paid to Valeant Pharmaceuticals. D.H. is a consultant for Allergan, Genetech, and Omeicos Therapeutics and has received financial support from the National Eye Institute, Lions VisionGift, Commonwealth Grant, Lions International, Syneos LLC, and the Macula Society. L.A.K. holds a patent (11229662) and has a patent pending (WO2019099595) related to ocular angiogenesis. L.A.K. also reports grants from CureVac, stock options from Ingenia Therapeutics and Pykus Therapeutics, outside the submitted work. N.A.P. is a consultant for Atheneum, Alcon, Allergan, Alimera, Eyepoint, Lifesciences, Guidepoint, and GLG. J.B.M. is a consultant for Alcon, Allergan, Carl Zeiss, Sunovion, Topcon, and Genentech. All other authors have reported that they have no relationships relevant to the contents of this paper to disclose.

References

1. Spaide RF, Jaffe GJ, Sarraf D, et al. Consensus nomenclature for reporting neovascular age-related macular degeneration data: consensus on neovascular age-related macular degeneration nomenclature study group. *Ophthalmology*. 2020;127(5):616–636. doi:10.1016/j.ophtha.2019.11.004
2. Wong WL, Su X, Li X, et al. Global prevalence of age-related macular degeneration and disease burden projection for 2020 and 2040: a systematic review and meta-analysis. *Lancet Glob Health*. 2014;2(2):e106–116. doi:10.1016/S2214-109X(13)70145-1
3. Zou M, Wang S, Chen A, et al. Prevalence of myopic macular degeneration worldwide: a systematic review and meta-analysis. *Br J Ophthalmol*. 2020;104(12):1748–1754. doi:10.1136/bjophthalmol-2019-315298
4. Wang JC, McKay KM, Sood AB, Laíns I, Sobrin L, Miller JB. Comparison of choroidal neovascularization secondary to white dot syndromes and age-related macular degeneration by using optical coherence tomography angiography. *Clin Ophthalmol*. 2019;13:95–105. doi:10.2147/OPTH.S185468
5. Ohno-Matsui K, Wu P-C, Yamashiro K, et al. IMI pathologic myopia. *Invest Ophthalmol Vis Sci*. 2021;62(5):5. doi:10.1167/iovs.62.5.5
6. Otsu N. A threshold selection method from gray-level histograms. *IEEE Trans Syst Man Cybern*. 1979;9(1):62–66. doi:10.1109/TSMC.1979.4310076
7. Schindelin J, Arganda-Carreras I, Frise E, et al. Fiji: an open-source platform for biological-image analysis. *Nat Methods*. 2012;9(7):676–682. doi:10.1038/nmeth.2019
8. Zudaire E, Gambardella L, Kurcz C, Vermeren S. A computational tool for quantitative analysis of vascular networks. *PLoS One*. 2011;6(11):e27385. doi:10.1371/journal.pone.0027385
9. Miere A, Butori P, Cohen SY, et al. Vascular remodeling of choroidal neovascularization after anti-vascular endothelial growth factor therapy visualized on optical coherence tomography angiography. *Retina*. 2019;39(3):548–557. doi:10.1097/IAE.0000000000001964
10. Coscas GJ, Lupidi M, Coscas F, Cagini C, Souied EH. optical coherence tomography angiography versus traditional multimodal imaging in assessing the activity of exudative age-related macular degeneration: a new diagnostic challenge. *Retina*. 2015;35(11):2219–2228. doi:10.1097/IAE.0000000000000766
11. Tokoro T. Types of fundus changes in the posterior pole. In: *Atlas of Posterior Fundus Changes in Pathologic Myopia*. Tokyo: Springer; 1998.
12. Baba T, Ohno-Matsui K, Yoshida T, et al. Optical coherence tomography of choroidal neovascularization in high myopia. *Acta Ophthalmol Scand*. 2002;80(1):82–87. doi:10.1034/j.1600-0420.2002.800116.x
13. Lains I, Wang JC, Cui Y, et al. Retinal applications of swept source optical coherence tomography (OCT) and optical coherence tomography angiography (OCTA). *Prog Retin Eye Res*. 2021;84:100951. doi:10.1016/j.preteyeres.2021.100951
14. Neelam K, Cheung CM, Ohno-Matsui K, Lai TY, Wong TY. Choroidal neovascularization in pathological myopia. *Prog Retin Eye Res*. 2012;31(5):495–525. doi:10.1016/j.preteyeres.2012.04.001
15. Leveziel N, Caillaux V, Bastuji-Garin S, Zmuda M, Souied EH. Angiographic and optical coherence tomography characteristics of recent myopic choroidal neovascularization. *Am J Ophthalmol*. 2013;155(5):913–919. doi:10.1016/j.ajo.2012.11.021
16. Parodi MB. Angiographic features after photodynamic therapy for choroidal neovascularisation in age related macular degeneration and pathological myopia. *Br J Ophthalmol*. 2003;87(2):177–183. doi:10.1136/bjo.87.2.177
17. Verteporfin in Photodynamic Therapy Study G. Photodynamic therapy of subfoveal choroidal neovascularization in pathologic myopia with verteporfin. 1-year results of a randomized clinical trial--VIP report no. 1. *Ophthalmology*. 2001;108(5):841–852. doi:10.1016/S0161-6420(01)00544-9

18. Onishi Y. Myopic macular neovascularization (diagnosis). In: Ohno-Matsui K, editor. *Atlas of Pathologic Myopia*. Singapore: Springer Singapore; 2020:61–67.
19. Yoshida T, Ohno-Matsui K, Ohtake Y, et al. Long-term visual prognosis of choroidal neovascularization in high myopia: a comparison between age groups. *Ophthalmology*. 2002;109(4):712–719. doi:10.1016/S0161-6420(01)01007-7
20. Lumbroso B, Rispoli M, Savastano MC. longitudinal optical coherence tomography-angiography study of type 2 naive choroidal neovascularization early response after treatment. *Retina*. 2015;35(11):2242–2251. doi:10.1097/IAE.0000000000000879
21. Avila MP, Weiter JJ, Jalkh AE, Trempe CL, Pruett RC, Schepens CL. Natural history of choroidal neovascularization in degenerative myopia. *Ophthalmology*. 1984;91(12):1573–1581. doi:10.1016/S0161-6420(84)34116-1
22. Friedenwald JS. Contribution to the theory and practice of tonometry. *Am J Ophthalmol*. 1937;20(10):985–1024. doi:10.1016/S0002-9394(37)90425-2
23. Seko Y, Seko Y, Fujikura H, Pang J, Tokoro T, Shimokawa H. Induction of vascular endothelial growth factor after application of mechanical stress to retinal pigment epithelium of the rat in vitro. *Invest Ophthalmol Vis Sci*. 1999;40(13):3287–3291.
24. Wong CW, Phua V, Lee SY, Wong TY, Cheung CM. Is choroidal or scleral thickness related to myopic macular degeneration? *Invest Ophthalmol Vis Sci*. 2017;58(2):907–913. doi:10.1167/iovs.16-20742
25. Wong CW, Teo YCK, Tsai STA, et al. Characterization of the choroidal vasculature in myopic maculopathy with optical coherence tomographic angiography. *Retina*. 2019;39(9):1742–1750. doi:10.1097/IAE.0000000000002233
26. Leveziel N, Yu Y, Reynolds R, et al. Genetic factors for choroidal neovascularization associated with high myopia. *Invest Ophthalmol Vis Sci*. 2012;53(8):5004–5009. doi:10.1167/iovs.12-9538
27. Ambati J, Fowler BJ. Mechanisms of age-related macular degeneration. *Neuron*. 2012;75(1):26–39. doi:10.1016/j.neuron.2012.06.018
28. Grunwald JE, Metelitsina TI, Dupont JC, Ying GS, Maguire MG. Reduced foveolar choroidal blood flow in eyes with increasing AMD severity. *Invest Ophthalmol Vis Sci*. 2005;46(3):1033–1038. doi:10.1167/iovs.04-1050
29. Boltz A, Luksch A, Wimpissinger B, et al. Choroidal blood flow and progression of age-related macular degeneration in the fellow eye in patients with unilateral choroidal neovascularization. *Invest Ophthalmol Vis Sci*. 2010;51(8):4220–4225. doi:10.1167/iovs.09-4968
30. McLeod DS, Grebe R, Bhutto I, Merges C, Baba T, Lutty GA. Relationship between RPE and choriocapillaris in age-related macular degeneration. *Invest Ophthalmol Vis Sci*. 2009;50(10):4982–4991. doi:10.1167/iovs.09-3639
31. Friedman DS, O'Colmain BJ, Munoz B, et al. Prevalence of age-related macular degeneration in the United States. *Arch Ophthalmol*. 2004;122(4):564–572.
32. Querques L, Giuffre C, Corvi F, et al. Optical coherence tomography angiography of myopic choroidal neovascularisation. *Br J Ophthalmol*. 2017;101(5):609–615. doi:10.1136/bjophthalmol-2016-309162
33. Battista M, Sacconi R, Borrelli E, et al. Discerning between macular hemorrhages due to macular neovascularization or due to spontaneous bruch's membrane rupture in high myopia: a comparative analysis between octa and fluorescein angiography. *Ophthalmol Ther*. 2022;11(2):821–831. doi:10.1007/s40123-022-00484-0
34. Soomro T, Talks J. The use of optical coherence tomography angiography for detecting choroidal neovascularization, compared to standard multimodal imaging. *Eye*. 2018;32(4):661–672. doi:10.1038/eye.2018.2
35. Eandi CM, Ciardella A, Parravano M, et al. Indocyanine green angiography and optical coherence tomography angiography of choroidal neovascularization in age-related macular degeneration. *Invest Ophthalmol Vis Sci*. 2017;58(9):3690–3696. doi:10.1167/iovs.17-21941
36. Wong TY, Ohno-Matsui K, Leveziel N, et al. Myopic choroidal neovascularisation: current concepts and update on clinical management. *Br J Ophthalmol*. 2015;99(3):289–296. doi:10.1136/bjophthalmol-2014-305131